Journal of Molecular Spectroscopy 364 (2019) 111179

Contents lists available at ScienceDirect

Journal of Molecular Spectroscopy

journal homepage: www.elsevier.com/locate/jms

Millimeter-wave spectroscopy of the chlorine isotopologues of chloropyrazine and twenty-two of their vibrationally excited states

Phoenix M. Higgins, Brian J. Esselman, Maria A. Zdanovskaia, R. Claude Woods *, Robert J. McMahon *

Department of Chemistry, University of Wisconsin–Madison, 1101 University Avenue, Madison, WI 53706-1322, United States

ARTICLE INFO

Article history:
Received 26 June 2019
In revised form 1 August 2019
Accepted 3 August 2019
Available online 5 August 2019

Keywords:
Chloropyrazine
Millimeter-wave
Rotational spectroscopy
Vibration-rotation interaction
Centrifugal distortion

ABSTRACT

The measurement of over 24,000 new rotational transitions of chloropyrazine ($C_4H_3N_2Cl$, μ_a = 1.55 D, μ_b = 0.14 D) in the 130–375 GHz frequency region enabled the assignments of the rotational spectra for the ground vibrational states of the [^{35}Cl]- and [^{37}Cl]-isotopologues and a combined total of 22 low-energy excited vibrational states. These vibrational states have been fit to sextic A-reduced Hamiltonians with low error (<0.05 MHz). These data allow for precise determination of the vibration-rotation interaction constants for the six lowest-energy fundamental vibrational modes (ν_{24}, ν_{17}, ν_{23}, ν_{16}, ν_{22}, and ν_{15}) of the [^{35}Cl]-isotopologue and the four lowest-energy fundamental vibrational modes (ν_{24}, ν_{17}, ν_{23}, and ν_{16}) of the [^{37}Cl]-isotopologue. In addition, many combination and overtone states were observed, bringing the total number of excited states to seventeen for the [^{35}Cl]-isotopologue and five for the [^{37}Cl]-isotopologue. The spectroscopic constants for the ground state, ν_{24}, and ν_{17} for each isotopologue are very well determined (N_{lines} > 1400 for each least-squares fit). The vibration-rotation interaction constants experimentally determined for all observed fundamentals are generally in quite close agreement with their predicted (B3LYP/6-311+G(2d,p)) values.

1. Introduction

Chloropyrazine ($C_4H_3N_2Cl$, Fig. 1) is a planar, near-prolate asymmetric top (κ = –0.854, μ_a = 1.55 D, μ_b = 0.14 D, B3LYP/6-311+(2d,p)). Previously, we have investigated the rotational spectra of the dinitrogen benzene analogues pyridazine (*ortho*-$C_4H_4N_2$) [1] and pyrimidine (*meta*-$C_4H_4N_2$), which are shown in Fig. 2. The pure rotational spectrum of pyrazine (*para*-$C_4H_4N_2$, Fig. 2), however, is unavailable due to the lack of a permanent dipole caused by the symmetrical substitution pattern of the ring. In chloropyrazine, chlorine atom substitution of pyrazine at any of the four equivalent carbon atoms breaks the symmetry of the ring, creating a permanent dipole moment. The σ_{C-Cl} bond lies nearly along the *a* principal axis, resulting in a rotational spectrum dominated by *a*-type transitions and very little change to the principal axes and their associated dipole moments upon chlorine isotopic substitution (Fig. 1).

Several studies of the rotational spectra of mono-chlorinated benzene derivatives have been reported previously; of particular relevance to the current work are the previous studies of chlorobenzene [2], 2-, 3-, and 4-chloropyridine [3–5], 2-chloropyrimidine [6], and chloropyrazine [7,8]. As expected, in each of these works, both the [^{35}Cl]- and [^{37}Cl]-isotopologues were observable at natural abundance. The spectra of vibrationally excited states were not reported for chlorobenzene, the chloropyridines, or chloropyrazine, despite at least one vibrationally excited state of the [^{35}Cl]-isotopologue having expected intensity greater than the [^{37}Cl]-isotopologue. The rotational constants of five vibrationally excited states were, however, reported for [^{35}Cl]-2-chloropyrimidine [6]. The spectra of three of these vibrationally excited states were assigned to ν_{16} (B_1), $2\nu_{16}$, and ν_{24} (B_2); two vibrationally excited states that were analyzed remained unassigned to specific vibrations.

Only two spectroscopic investigations of chloropyrazine have been previously reported [7–9]. The condensed-phase and gas-phase Raman and infrared spectra were obtained by Endrédi et al. [9], who measured the fundamental vibrational modes for pyrazine, chloropyrazine, and 2,6-dichloropyrazine. The gas-phase rotational spectrum of chloropyrazine has been studied previously from 8 to 38 GHz by Akavipat et al. [7,8], and that work provided the rotational constants of the ground state of [^{35}Cl]- and [^{37}Cl]-chloropyrazine. Since the previous microwave work was limited to less than 40 GHz, all of the R-branch transitions measured were less than J' = 14. Isotopologues containing ^{35}Cl and ^{37}Cl were observed at their natural abundance, but spectra of vibrationally excited states were not reported. Due to the limited data sets (71 transitions for [^{35}Cl]-chloropyrazine and 55 transi-

* Corresponding authors.
E-mail addresses: rcwoods@wisc.edu (R.C. Woods), robert.mcmahon@wisc.edu (R.J. McMahon).

https://doi.org/10.1016/j.jms.2019.111179
0022-2852/

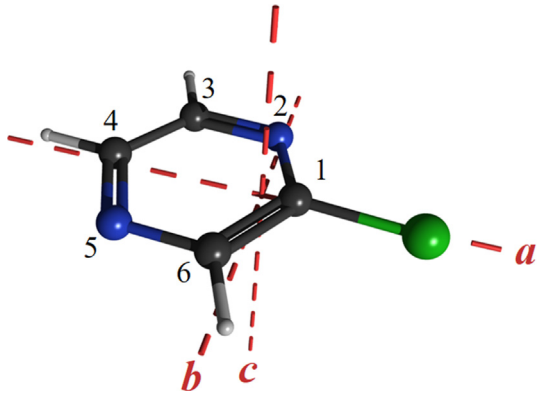

Fig. 1. [^{35}Cl]-Chloropyrazine structure (B3LYP/6-311+G(2d,p)) with principal rotation axes and atom numbering. The dipole moment components are μ_a = 1.55 D and μ_b = 0.14 D.

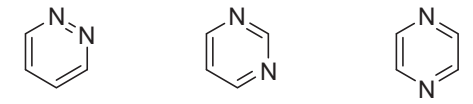

Fig. 2. The three regioisomeric dinitrogen analogs of benzene, pyridazine (*ortho*-$C_4H_4N_2$), pyrimidine (*meta*-$C_4H_4N_2$), and pyrazine (*para*-$C_4H_4N_2$).

tions for [^{37}Cl]-chloropyrazine), only the rotational constants and two quartic centrifugal distortion constants (Δ_J and Δ_{JK}) could be determined from the least-squares fitting of an A-reduced Hamiltonian (Table 1). A subset of the transitions reported in the original study [7] with *obs.* – *calc.* < 0.150 MHz were included in the data set of the current work. In that low frequency range, hyperfine-resolved transitions were observed due to the chlorine nucleus, though the frequencies of their transitions were not reported.

In the current study, we have analyzed the rotational spectra of both chlorine isotopologues of chloropyrazine in their ground vibrational states and a total of 22 vibrationally excited states. Each has been least-squares fit to an A-reduced, sextic single-state model. We have provided a detailed analysis of each state and a comparison to computational results. Finally, we have made some comparisons of the results to those of previously published haloarenes.

Table 1
Spectroscopic constants for [^{35}Cl]- and [^{37}Cl]-chloropyrazine (A-reduced Hamiltonian, I^r representation) derived from previous work [7,8].

	[^{35}Cl]	[^{37}Cl]
$A_0^{(A)}$ (MHz)	6042.281 (115)	6041.942 (103)
$B_0^{(A)}$ (MHz)	1664.099 (3)	1616.591 (3)
$C_0^{(A)}$ (MHz)	1304.622 (3)	1275.234 (3)
Δ_J (kHz)	0.0723 (103)	0.0516 (84)
Δ_{JK} (kHz)	0.3545 (171)	0.3476 (134)
N_{lines}	71	55
σ	0.09	0.07
Δ_i (uÅ^2)	0.0401 (19)	0.0376 (18)
κ	−0.848	−0.857
χ_{aa} Cl (MHz)	−71.64 (13)	−56.67 (32)
χ_{bb} Cl (MHz)	40.48[a]	
χ_{cc} Cl (MHz)	31.16[a]	

[a] Calculated using the published value of $\eta = \frac{\chi_{bb}-\chi_{cc}}{\chi_{aa}}$ (no error limits provided) and the relation $\chi_{aa} + \chi_{bb} + \chi_{cc} = 0$.

2. Experimental and theoretical methods

The rotational spectrum presented in this work from 130 to 375 GHz was generated using a millimeter-wave and submillimeter-wave spectrometer, which has been previously described [1,10,11]. Chloropyrazine (Sigma-Aldrich, 98% purity) was used without further purification at a sample pressure of 4.0 mTorr in a continuous flow. The continuous 130–230 GHz and 235–375 GHz spectral segments, in combination with the convenient AABS package [12,13], including ASFIT and ASROT [14], allowed for a very large number of rotational transitions (N_{lines} > 500) to be measured and analyzed for most of the vibrational states and isotopic forms studied in this work. In total, frequencies of over 24,000 independent transitions were measured, least-squares fit, and are reported here. For all states reported in this work, a sextic A-reduced Hamiltonian, I^r representation, was necessary to fit the observed spectrum. In an attempt to obtain spectroscopic constants that are fairly free of perturbation and close to their true values, we fixed distortion terms that could not be adequately determined from a particular least-squares fit as described below. For the ground state sextic constants that could not be satisfactorily fit, B3LYP/6-311+(2d,p) computed values were used. Ground state constant values were used for all least-squares fits of fundamental states where sextic or quartic terms could not be determined. For overtone or combination states, extrapolated distortion constants using polynomial fits were used when those terms could not be directly determined for that state. Because several of the vibrational states may be coupled to one another and had differing numbers of available transitions, distortion constants that varied by more than an order of magnitude from the expected value or changed sign were fixed. When extrapolation of a distortion constant for an overtone or combination state resulted in a change of sign for that term, the distortion constant was set to zero. Measured transition frequencies that had *obs.* – *calc.* values greater than 0.1 MHz in their least-squares fits were excluded from the data set. All files associated with the least-squares fitting and prediction of these spectra are available in the Supplementary Material.

The B3LYP/6-311 + G(2d,p) geometry optimizations and anharmonic frequency calculations were carried out in Gaussian 16 [15] with the WebMO interface [16] for both isotopologues. Calculations were performed with very tight convergence criteria (opt = verytight int = grid = ultrafine), which afforded sufficiently accurate quartic and sextic distortion constants, fundamental vibrational frequencies, and vibration-rotation interaction constants. Table 2 provides the computed frequencies of the six lowest-energy fundamental vibrational modes of [^{35}Cl]-chloropyrazine and the four lowest-energy fundamental vibrational modes of [^{37}Cl]-chloropyrazine with their predicted vibration-rotation interaction constants. Fig. 3 displays the fundamental vibrational states of [^{35}Cl]-chloropyrazine below 800 cm^{-1} observed by Endrédi et al. [9] along with the predicted overtone and combination states. The rotational transitions of all these vibrational states were observed, measured, and least-squares fit in this work, with the exception of fundamentals ν_{14} and ν_{21}. To assign the vibrational states of [^{35}Cl]-2-chloropyrimidine, an anharmonic frequency calculation was performed in the same manner as described above. The output files of each theoretical calculation and analysis are provided in the Supplementary Material.

3. Spectral and computational analysis

The rotational spectrum of chloropyrazine (Fig. 4) is dominated by intense $^aR_{0,1}$ transitions due to its overall dipole moment lying very near the *a*-axis (Fig. 1). The component dipole μ_a is ~10× lar-

Table 2
Experimental and computed values of lowest-energy fundamental vibrations, and computed vibration-rotation interaction constants, for chloropyrazine.

	Mode	Symmetry	Experimental (cm^{-1})[a]	Rotational Transition Intensities at 298 K[b]	B3LYP/6–311+(2d,p) Fundamental Frequency (cm^{-1})	$A_0 - A_v$ (MHz)	$B_0 - B_v$ (MHz)	$C_0 - C_v$ (MHz)
[^{35}Cl]	ν_{15}	A′	618	0.05	623.2	0.60	0.20	0.94
	ν_{22}	A″	477	0.10	488.7	1.69	0.12	−0.67
	ν_{16}	A′	435	0.12	420.4	−0.44	1.99	1.04
	ν_{23}	A″	413	0.13	418.3	4.45	−0.12	−0.70
	ν_{17}	A′	309	0.22	302.2	−25.97	−0.06	1.05
	ν_{24}	A″	188	0.40	167.1	29.16	−1.08	−1.56
[^{37}Cl]	ν_{16}	A′	435	0.04	413.4	−0.43	1.94	1.02
	ν_{23}	A″	413	0.04	418.2	4.58	−0.16	−0.72
	ν_{17}	A′	309	0.07	299.9	−26.19	−0.05	−1.03
	ν_{24}	A″	188	0.14	166.4	29.38	−1.06	−1.52

[a] Experimental infrared or Raman fundamental frequencies measured from a mixture of natural abundance chloropyrazine isotopologues [9].
[b] Relative to [^{35}Cl]-chloropyrazine ground vibrational state.

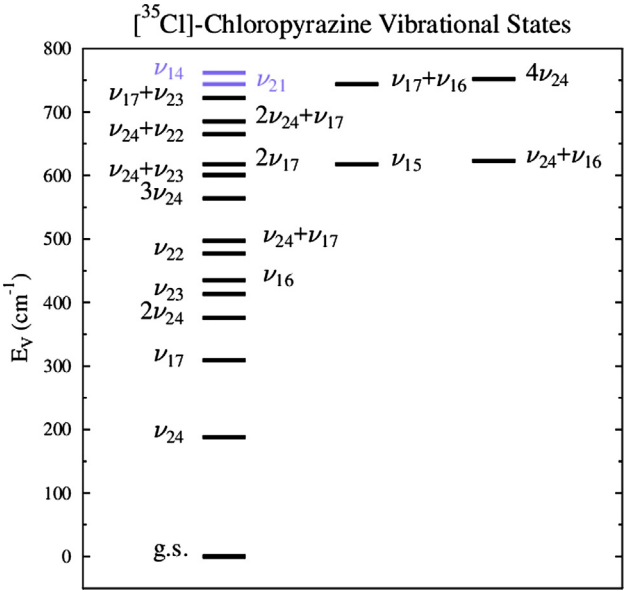

Fig. 3. Vibrational energy levels of [^{35}Cl]-chloropyrazine below 800 cm^{-1}, drawn from experimental fundamental frequencies reported by Endrédi et al. [9]. Fundamentals ν_{14} and ν_{21} are in slate blue as their rotational transitions were not measured and least-squares fit in this work. (For interpretation of the references to colour in this figure legend, the reader is referred to the web version of this article.)

ger than the magnitude of μ_b, which results in a ~100× intensity difference of the *a*-type and *b*-type transitions. Due to the spectral density apparent in Fig. 4, no *b*-type transitions were observed at such low intensity relative to the intensity of *a*-type transitions of other vibrationally excited states.

No P- or Q-branch transitions were observed due to their low intensities throughout the frequency range examined. While the previous work was limited in its ability to predict transitions in the mm-wave range due to the lack of accurate quartic distortion terms, it did provide excellent estimates of the A_0, B_0, and C_0 rotational constants. Thus, the band structure of the $K_a = 0$ transitions of the $^aR_{0,1}$ bands, spaced by approximately 2600 MHz (~2*C*), and their general line spacing within a band at low K_a, were well predicted from the previous microwave study [7,8]. The $^aR_{0,1}$ subbands begin with transitions that have the same values of *J* and K_c, but two different values of K_a, in the frequency range examined. The quantum numbers for the degenerate transitions are thus $K_a + K_c = J$ and $K_a + K_c = J + 1$. Transitions within the subbands spread out to higher frequency with increasing K_a and concurrently decreasing *J*. The K_c-degenerate pairs of transitions lose degeneracy as K_a increases. At high values of K_a and lower values of K_c, there are degenerate pairs of transitions with equal values of K_a, but different values of K_c.

3.1. [^{35}Cl]-Chloropyrazine, vibrational ground state

While the rotational constants of Akavipat et al. [7,8] are close to those determined in this work (Table 3), the lack of accurate sextic and quartic centrifugal distortion constants results in errors in the predictions of the lead R-branch transition frequencies (K_a = 0,1 oblate-degenerate series) of up to 428 MHz in the 130–375 GHz region. A simple replacement of all quartic distortion constants from the previous work with those calculated at the B3LYP/6-311 + G(2d,p) level of theory (Table 3), reduces the error in prediction of the lead transition frequencies to approximately 6 MHz. Due to the low dependence of the lead R-branch transitions on the sextic centrifugal distortion constants, the inclusion of B3LYP-calculated values does not improve the prediction of these transitions. The final data set of the vibrational ground state of [^{35}Cl]-chloropyrazine consists of 3573 newly measured independent transitions and 53 independent transitions from the previous microwave work. A data distribution plot is provided in Fig. 5, demonstrating the breadth of the set of measured transitions and low error in the measurements. The data set includes transitions from J'' = 3 to 130 and K_a'' = 0 to 73. Assuming an experimental error of 80 kHz for the microwave transitions and 50 kHz for the mm-wave transitions, any transitions with *obs.* − *calc.* values greater than two times the experimental error value were eliminated from the data set. In such a dense spectrum, accidental overlapping signals from ground state [^{35}Cl]-chloropyrazine, [^{37}Cl]-chloropyrazine, and their vibrational satellites greatly reduce the number of transitions that can be measured precisely. In the lower frequency range (130 – 230 GHz), many transitions (N_{lines} > 500) displayed splitting due to nuclear quadrupole coupling to the chlorine substituent. These transitions were excluded from the data set that produced the constants displayed in Table 3. A separate least-squares fit including the hyperfine-resolved transitions did not produce a better determination of the nuclear quadrupole coupling constants than the previous work [7,8]. In the frequency range of this work, many transitions that are hyperfine-resolved due to the chlorine nucleus are visible in which the quartet of transitions (where $F = J + \frac{1}{2}, J - \frac{1}{2}, J + \frac{3}{2}$, and $J - \frac{3}{2}$) has collapsed into doublets ($F = J \pm \frac{1}{2}$ and $J \pm \frac{3}{2}$), though the splitting data from these doublets are insufficient to allow for refinement of the hyperfine constants.

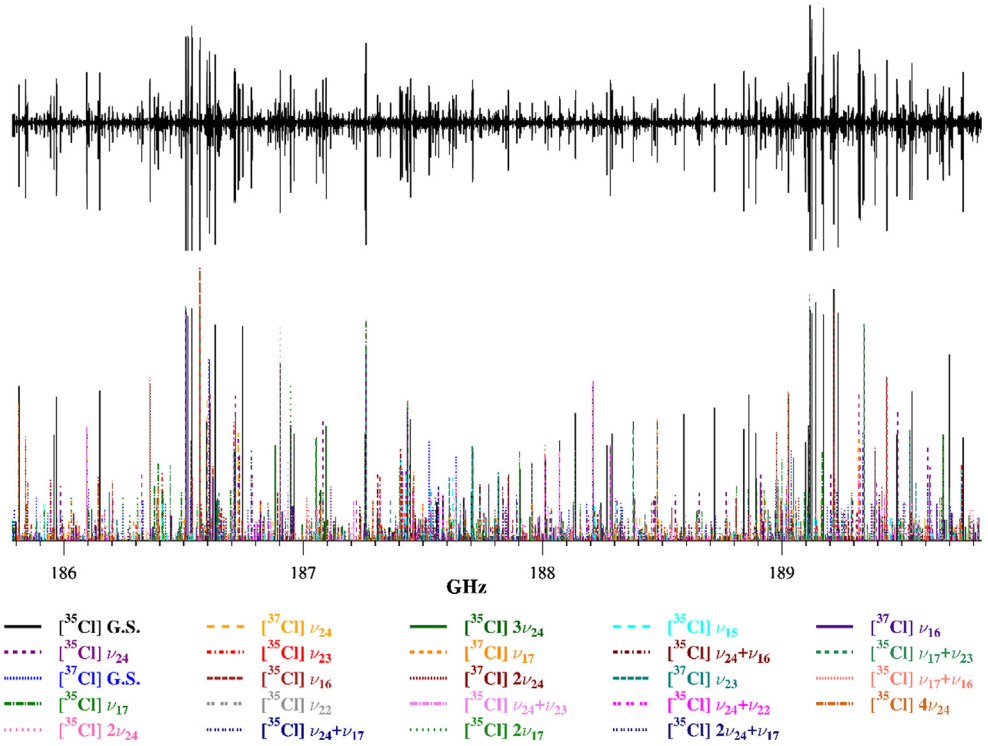

Fig. 4. Rotational spectrum of chloropyrazine from 185.8 to 189.8 GHz with predicted stick spectra for [^{35}Cl]- and [^{37}Cl]-chloropyrazine ground and vibrationally excited states.

The least-squares fitting of 3626 independent transitions of ground state [^{35}Cl]-chloropyrazine to a sextic distorted-rotor Hamiltonian resulted in an excellent determination of its rotational constants (Table 3). The value of $A_0^{(A)}$ is the most poorly determined of the rotational constants due to the limitation of the data set to ^{a}R-branch transitions, though it is still determined to an accuracy of 1.5 kHz due to the very large data set. Least-squares fitting of the same large data set of $^aR_{0,1}$ transitions, however, determines the values of $B_0^{(A)}$ and $C_0^{(A)}$ to a remarkable statistical precision of less than 60 Hz. The computational predictions of these values were reasonable, with errors in $A_0^{(A)}$, $B_0^{(A)}$, and $C_0^{(A)}$ of 0.4%, 1.5%, and 1.1%, respectively. This computational error in $C_0^{(A)}$, however,

Table 3
Spectroscopic constants for [^{35}Cl]-chloropyrazine and its vibrationally excited states (A-reduced Hamiltonian, I^r representation).

	B3LYP/6–311+(2d,p) [^{35}Cl] G.S.	Current work[a] [^{35}Cl] G.S.	ν_{24}[b] A″, 188 cm^{-1}	ν_{17}[b] A′, 309 cm^{-1}	$2\nu_{24}$ A′, 376 cm^{-1}
$A_v^{(A)}$ (MHz)	6065	6042.0319 (14)	6013.3983 (17)	6067.1385 (16)	5985.5091 (13)
$B_v^{(A)}$ (MHz)	1639	1664.102005 (53)	1665.219176 (64)	1664.217380 (50)	1666.335583 (46)
$C_v^{(A)}$ (MHz)	1290	1304.611805 (49)	1306.194813 (60)	1303.657460 (40)	1307.773362 (36)
Δ_J (kHz)	0.0678	0.0670483 (10)	0.0676588 (13)	0.0672151 (12)	0.0682848 (13)
Δ_{JK} (kHz)	0.334	0.334847 (15)	0.338036 (23)	0.329432 (48)	0.340584 (38)
Δ_K (kHz)	1.03	1.0569 (20)	0.8631 (24)	1.2732 (28)	0.6887 (17)
δ_J (kHz)	0.0158	0.0158818 (19)	0.0159590 (23)	0.0159287 (93)	0.01603562 (70)
δ_K (kHz)	0.350	0.348712 (95)	0.33577 (11)	0.36531 (13)	0.323533 (48)
Φ_J (Hz)	0.000000207	[0.0000002067][c]	[0.0000002067][c,d]	[0.0000002067][c,d]	[0.0000002067][c,d]
Φ_{JK} (Hz)	0.000142	0.0001363 (79)	0.0000935 (99)	0.000157 (11)	0.0000500 (16)
Φ_{KJ} (Hz)	−0.000606	−0.000593 (27)	−0.000235 (33)	−0.000902 (42)	−0.000155 (93)
Φ_K (Hz)	0.00142	[0.001421][c]	[0.001421][c,d]	[0.001421][c,d]	[0.001421][c,d]
φ_J (Hz)	0.000000711	0.000000666 (59)	0.000000634 (72)	[0.000000666][d]	[0.0000006028][e]
φ_{JK} (Hz)	0.0000671	0.0000240 (35)	0.0000258 (44)	0.0000441 (56)	[0.00002777][e]
φ_K (Hz)	0.00196	0.00174 (13)	0.00092 (16)	0.00192 (19)	[0.0001108][e]
N_{lines}		3626	2929	2169	1979
σ		0.033	0.037	0.038	0.039
Δ_i (uÅ^2)	0.053	0.040228 (26)	−0.623783 (32)	0.690993 (27)	−1.279060 (23)
κ	−0.854	−0.848	−0.847	−0.849	−0.847
χ_{aa} Cl (MHz)	−67.9				
χ_{bb} Cl (MHz)	28.7				
χ_{cc} Cl (MHz)	39.3				

Table 3 *(continued)*

	ν_{23}[b] A″, 413 cm^{-1}	ν_{16}[b] A′, 435 cm^{-1}	ν_{22}[b] A″, 477 cm^{-1}	$\nu_{24}+\nu_{17}$ A″, 497 cm^{-1}	$3\nu_{24}$ A″, 564 cm^{-1}
$A_v^{(A)}$ (MHz)	6037.4592 (15)	6041.6598 (18)	6040.527 (55)	6038.800 (58)	5958.3577 (93)
$B_v^{(A)}$ (MHz)	1664.263213 (53)	1662.571178 (52)	1664.0977 (46)	1665.1593 (48)	1667.44719 (91)
$C_v^{(A)}$ (MHz)	1305.352003 (41)	1303.769583 (44)	1305.294465 (68)	1305.248771 (67)	1309.347445 (47)
Δ_J (kHz)	0.0672266 (16)	0.0676067 (16)	0.06530 (25)	0.06850 (37)	0.068666 (45)
Δ_{JK} (kHz)	0.334564 (63)	0.333503 (30)	0.412 (11)	0.308 (15)	0.3495 (19)
Δ_K (kHz)	1.0606 (20)	1.0295 (24)	[1.0569][d]	[1.079][e]	[0.5337][e]
δ_J (kHz)	0.01591085 (85)	0.01604780 (86)	0.01490 (12)	0.01638 (18)	0.015982 (22)
δ_K (kHz)	0.347736 (55)	0.347928 (71)	0.3583 (22)	0.3534 (28)	0.31182 (44)
Φ_J (Hz)	[0.0000002067][c,d]	[0.0000002067][c,d]	[0.0000002067][c,d]	[0.0000002067][c,d]	[0.0000002067][c,d]
Φ_{JK} (Hz)	0.0001377 (29)	[0.0001363][d]	[0.0001363][d]	[0.0001151][e]	[0.000005981][e]
Φ_{KJ} (Hz)	[−0.0005931][d]	[−0.0005931][d]	[−0.0005931][d]	[−0.0005446][e]	[0.0][f]
Φ_K (Hz)	[0.001421][c,d]	[0.001421][c,d]	[0.001421][c,d]	[0.001421][c,d]	[0.001421][c,d]
φ_J (Hz)	[0.0000006664][d]	[0.0000006664][d]	[0.0000006664][d]	[0.0000006346][e]	[0.0000005710][e]
φ_{JK} (Hz)	[0.00002401][d]	[0.00002401][d]	[0.00002401][d]	[0.00004606][e]	[0.00002964][e]
φ_K (Hz)	[0.001747][d]	[0.001747][d]	[0.001747][d]	[0.001106][e]	[0.0][f]
N_{lines}	1672	1312	401	341	618
σ	0.039	0.044	0.046	0.043	0.042
Δ_i (uÅ^2)	−0.213368 (26)	0.005690 (30)	−0.1840 (11)	−0.0008 (12)	−1.92620 (21)
κ	−0.848	−0.849	−0.848	−0.848	−0.846

	$\nu_{24}+\nu_{23}$ A′, 601 cm^{-1}	ν_{15}[b] A′, 618 cm^{-1}	$2\nu_{17}$ A′, 618 cm^{-1}	$\nu_{24}+\nu_{16}$ A″, 623 cm^{-1}	$\nu_{24}+\nu_{22}$ A′, 665 cm^{-1}
$A_v^{(A)}$ (MHz)	6006.61 (58)	6042.68 (23)	6092.18 (18)	6010.96 (13)	6011.69 (40)
$B_v^{(A)}$ (MHz)	1666.554 (46)	1663.759 (19)	1664.335 (14)	1663.757 (11)	1665.233 (32)
$C_v^{(A)}$ (MHz)	1306.83008 (10)	1303.78457 (11)	1302.680235 (69)	1305.36512 (13)	1306.87357 (11)
Δ_J (kHz)	0.06814 (61)	0.06809 (10)	0.06780 (24)	0.06607 (42)	0.06453 (49)
Δ_{JK} (kHz)	0.318 (18)	[0.3348][d]	0.3159 (74)	0.405 (13)	0.461 (15)
Δ_K (kHz)	[0.8669][e]	[1.057][d]	[1.490][e]	[0.8358][e]	[0.8632][e]
δ_J (kHz)	0.01597 (30)	0.016409 (50)	0.01620 (12)	0.01504 (20)	0.01427 (24)
δ_K (kHz)	[0.3348][e]	0.3670 (20)	[0.3819][e]	[0.3350][e]	[0.3454][e]
Φ_J (Hz)	[0.0000002067][c,d]	[0.0000002067][c,d]	[0.0000002067][c,d]	[0.0000002067][c,d]	[0.0000002067][c,d]
Φ_{JK} (Hz)	[0.00009490][e]	[0.0001363][d]	[0.0001794][e]	[0.00009353][e]	[0.00009353][e]
Φ_{KJ} (Hz)	[−0.0002355][e]	[−0.0005931][d]	[−0.001211][e]	[−0.0002355][e]	[−0.0002355][e]
Φ_K (Hz)	[0.001421][c,d]	[0.001421][c,d]	[0.001421][c,d]	[0.001421][c,d]	[0.001421][c,d]
φ_J (Hz)	[0.0000006346][e]	[0.0000006664][d]	[0.0000006664][e]	[0.0000006346][e]	[0.0000006346][e]
φ_{JK} (Hz)	[0.00002589][e]	[0.00002401][d]	[0.00006435][e]	[0.00002589][e]	[0.00002589][e]
φ_K (Hz)	[0.0009289][e]	[0.001747][d]	[0.002102][e]	[0.0009289][e]	[0.0009289][e]
N_{lines}	122	154	265	182	127
σ	0.048	0.050	0.040	0.048	0.044
Δ_i (uÅ^2)	−0.664 (12)	0.2324 (47)	1.3456 (35)	−0.6787 (27)	−0.8461 (80)
κ	−0.847	−0.848	−0.849	−0.848	−0.848

	$2\nu_{24}+\nu_{17}$ A′, 685 cm^{-1}	$\nu_{17}+\nu_{23}$ A″, 722 cm^{-1}	$\nu_{17}+\nu_{16}$ A′, 744 cm^{-1}	$4\nu_{24}$ A′, 752 cm^{-1}
$A_v^{(A)}$ (MHz)	6009.7379 (25)	6062.5865 (81)	[6066.77][e]	5930.92 (21)
$B_v^{(A)}$ (MHz)	1665.355081 (90)	1664.39765 (24)	1662.5775 (40)	1668.638 (17)
$C_v^{(A)}$ (MHz)	1306.881873 (61)	1304.406075 (86)	1302.75937 (14)	1310.915657 (81)
Δ_J (kHz)	0.0679251 (58)	0.0673954 (42)	0.0677816 (49)	0.0685260 (32)
Δ_{JK} (kHz)	0.334050 (94)	0.33059 (64)	[0.3281][e]	0.37468 (77)
Δ_K (kHz)	0.9407 (66)	1.260 (31)	[1.246][e]	0.427 (77)
δ_J (kHz)	0.0159618 (30)	[0.01595][e]	[0.01609][e]	[0.01567][e]
δ_K (kHz)	0.33733 (15)	[0.3643][e]	[0.3645][e]	[0.3005][e]
Φ_J (Hz)	[0.0000002067][c,d]	[0.0000002067][c,d]	[0.0000002067][c,d]	[0.0000002067][c,d]
Φ_{JK} (Hz)	[0.00007192][e]	[0.0001592][e]	[0.0001579][e]	[0.0][f]
Φ_{KJ} (Hz)	[−0.0002558][e]	[−0.0009022][e]	[−0.0009022][e]	[0.0][f]
Φ_K (Hz)	[0.001421][c,d]	[0.001421][c,d]	[0.001421][c,d]	[0.001421][c,d]
φ_J (Hz)	[0.0000006028][e]	[0.0000006664][e]	[0.0000006664][e]	[0.0000005391][e]
φ_{JK} (Hz)	[0.00004793][e]	[0.00004418][e]	[0.00004418][e]	[0.00003152][e]
φ_K (Hz)	[0.0002882][e]	[0.001924][e]	[0.001924][e]	[0.0][f]
N_{lines}	723	136	28	266
σ	0.042	0.042	0.041	0.044
Δ_i (uÅ^2)	−0.853612 (43)	0.43886 (12)	0.654 (14)[g]	−1.92620 (21)
κ	−0.848	−0.849	−0.849	−0.846

[a] Least-squares fit including newly measured transitions and data from refs. [7,8].
[b] Vibrational frequencies from ref. [9].
[c] Value fixed to B3LYP/6-311+G(2d,p) computed value.
[d] Value fixed to ground state value.
[e] Value fixed based upon extrapolation from other vibrational states in its corresponding series.
[f] Constant fixed to zero because value extrapolated from other vibrational states in corresponding series would change sign relative to other values in series.
[g] An error of 1.0 MHz in the value of $A_{17,16}$ was assumed in calculating the inertial defect, Δ_i.

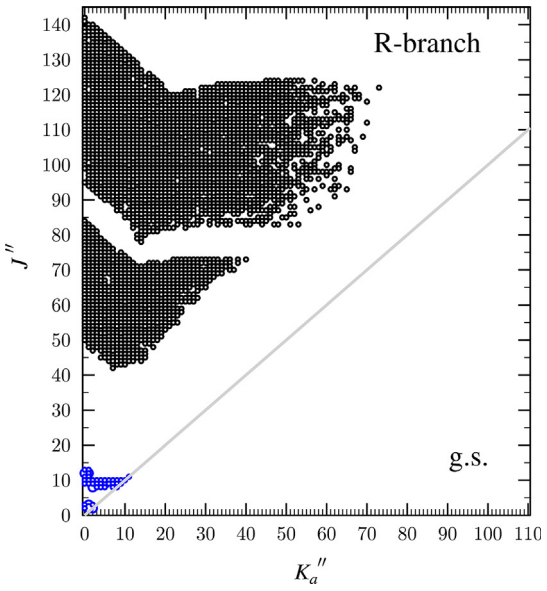

Fig. 5. Data distribution plot for the least-squares fit of spectroscopic data for ground state [^{35}Cl]-chloropyrazine from the current work (black circles) and measurements from Akavipat et al. [7,8] (blue circles) The size of the plotted circle is proportional to the value of $f_{obs.} - f_{calc.}$ and all values shown have errors smaller than twice the estimated experimental error of 50 kHz for the new data or 80 kHz for the previous measurements. Data distribution plots for all other states are available in the Supplementary Material. (For interpretation of the references to colour in this figure legend, the reader is referred to the web version of this article.)

translates into an absolute error of 14 MHz, which has a substantial impact on the ability of these constants to precisely predict the band origins of the $^{a}R_{0,1}$ transitions. A similar level of accuracy (0.2% to 2.4%) in the quartic centrifugal distortion constants was sufficient for them to be quite useful in the initial predictions, as stated previously. As a full set of sextic centrifugal distortion constants could not be determined, the accuracy of the B3LYP calculation of those constants is more difficult to assess. All of the experimentally determined sextic terms are of the same sign and magnitude with errors smaller than 12%, except for ϕ_{JK}, where the error is approximately 180%. Fixing ϕ_{JK} to its computed value increased the error of the fit and increased the error in all of the other quartic distortion terms, so ϕ_{JK} was allowed to fit in the final least-squares fit despite its seemingly high discrepancy from the computational prediction. As will be shown below, this choice was validated by the similar value of ϕ_{JK} obtained for ν_{24}.

3.2. [^{35}Cl]-Chloropyrazine, ν_{24} (v = 1, 2, 3, 4)

The lowest-energy vibrational mode ν_{24} (A″, 188 cm^{-1}) is a ring deformation involving an out-of-plane bending of the σ_{C-Cl} bond. For ν_{24}, many transitions were observable at 0.40 times the intensity of their corresponding ground state transitions. Combining the ground-state centrifugal distortion constants with rotational constants from the ground state that had been corrected for vibration–rotation interactions provided an excellent initial prediction of the K_a = 0,1 oblate-degenerate series. The final least-squares fit (sextic, distorted-rotor Hamiltonian) contained 2933 independent transitions, just slightly fewer than its ground vibrational state. Like the ground state, this least-squares fit determined all rotational, quartic centrifugal, and sextic centrifugal distortion terms, except the sextic on-diagonal (designated by capital subscripts), purely J- and K-dependent terms (Φ_J and Φ_K). These terms were fixed to the computed ground state values assuming that their true values were better approximated by the computed ground state values than by zero. The strong similarity between the values of ϕ_{JK} for the ground vibrational state and ν_{24} of [^{35}Cl]-chloropyrazine (2.40×10^{-11} MHz and 2.59×10^{-11} MHz, respectively) validates their inclusion in both ground and excited vibrational state fits despite the aforementioned deviation from the computed value. The experimentally determined vibration-rotation interaction constants ($B_0 - B_{24}$) and inertial defect and the corresponding computationally predicted values are presented in Table 4. As expected, the computed values are in excellent agreement with the experimental vibration-rotation interaction constants, with the largest magnitude error in the value of $A_0 - A_{24}$ (the experimental and computed values differ by 0.53 MHz, 1.8%). The ground state and ν_{24} of [^{35}Cl]-chloropyrazine least-squares fits provided the foundation for investigating the remaining states of the ν_{24} (v = 2, 3, 4) series.

The transitions of the two-quantum overtone $2\nu_{24}$ were easily predicted by extrapolation from the ground state and ν_{24} spectroscopic constants. In total, 1979 independent transitions for $2\nu_{24}$ were measured and least-squares fit. The reduced number of transitions allowed for determination of a sextic distorted-rotor Hamiltonian with only the on-diagonal J- and K-dependent sextic terms, Φ_{JK} and Φ_{KJ}, allowed to vary. For ν_{24} (v = 2, 3, 4), distortion constants that could not be determined *via* least-squares fitting of the available transitions, or were not consistent with extrapolated values from the lower-quanta states, were fixed. An extrapolated value was used when it had the same sign as the constants of the lower-energy states in its series. If the extrapolated value changed the sign of the distortion term, the corresponding constant was fixed to zero for the given vibrational state. This method allowed for satisfactory least-squares fits using a distorted-rotor Hamiltonian for ν_{24} (v = 2, 3, 4) with a reduction in the number of constants included in the fitting as the number of observable lines decreased. As can be seen in Fig. 6, the spectroscopic constants for the entire ν_{24} series display smooth changes as a function of the vibrational quantum number. Fig. 6a shows the changes in the rotational constants relative to the ground state constant as a function of vibrational excitation. The line for each is a polynomial model fit including each of the data points. Fig. 6b shows the change in the inertial defect upon vibrational excitation. The smoothness of these two data sets provides validation of all of these constants. Fig. 6c and d display the changes in centrifugal distortion constants as a function of vibrational excitation. All non-zero distortion constants are displayed; fixed constants are represented by open symbols. Trendlines were modeled from all determined constants in the series using an appropriate polynomial. The smooth progression of quartic distortion constant values (Fig. 6c) suggests that the experimentally determined values are physically meaningful. The purely J-dependent terms (Δ_J, δ_J) show a smaller change upon vibrational excitation than the purely K-dependent terms (Δ_K, δ_K). It is worth noting that ν_{24}, $2\nu_{24}$, and $3\nu_{24}$ are separated from their nearest vibrational neighbors by at least 35 cm^{-1}, whereas $4\nu_{24}$ is only 8 cm^{-1} and 10 cm^{-1} away from its nearest vibrational neighbors. The deviations observed in the $4\nu_{24}$ quartic distortion constants may thus be signs of unaddressed perturbation. In particular, Δ_{JK} and Δ_K show the greatest deviation from linearity and from the model. Interestingly, the value of Δ_K could not be satisfactorily determined for $3\nu_{24}$, but the value was necessary to fit for $4\nu_{24}$ to prevent high error and divergence of other quartic distortion terms from their expected values, again suggesting potential perturbation. The experimentally determined sextic centrifugal distortion constants (Fig. 6d) show similar trends to the quartic centrifugal distortion constants. The purely J-dependent term (ϕ_J) changes less than the purely K-dependent term (ϕ_K) upon vibrational excitation. The on-diagonal sextic terms that were least-squares fit for the first two quanta appear also to be reasonably meaningful physical quantities from their smooth progression, especially that of Φ_{JK}. The off-diagonal distortion con-

Table 4
Vibration-rotation interaction constants and inertial defects of chloropyrazine (A-reduced Hamiltonian, I^r representation).

	[^{35}Cl]-chloropyrazine		[^{37}Cl]-chloropyrazine	
	Experimental	B3LYP/6-311+(2d,p)	Experimental	B3LYP/6-311+(2d,p)
	ν_{24}		ν_{24}	
$A_0 - A_{24}$ (MHz)	28.6336 (22)	29.16	28.8587 (29)	29.38
$B_0 - B_{24}$ (MHz)	−1.117171 (83)	−1.08	−1.0990 (10)	−1.06
$C_0 - C_{24}$ (MHz)	−1.583008 (77)	−1.56	−1.543106 (92)	−1.52
Δ_i (uÅ^2)	−0.623783 (32)	−0.618	−0.627106 (56)	−0.622
	ν_{17}		ν_{17}	
$A_0 - A_{17}$ (MHz)	−25.1066 (21)	−25.97	−25.3281 (38)	−26.19
$B_0 - B_{17}$ (MHz)	−0.115375 (73)	−0.06	−0.10822 (11)	−0.05
$C_0 - C_{17}$ (MHz)	0.954345 (63)	1.05	0.932164 (95)	1.03
Δ_i (uÅ^2)	0.690993 (27)	0.740	0.700945 (55)	0.751
	ν_{23}		ν_{23}	
$A_0 - A_{23}$ (MHz)	4.5728 (21)	4.45	4.5837 (65)	4.47
$B_0 - B_{23}$ (MHz)	−0.161208 (75)	−0.12	−0.16328 (26)	−0.13
$C_0 - C_{23}$ (MHz)	−0.740197 (64)	−0.70	−0.715613 (92)	−0.68
Δ_i (uÅ^2)	−0.213368 (26)	−0.198	−0.21327 (10)	−0.198
	ν_{16}		ν_{16}	
$A_0 - A_{16}$ (MHz)	0.3721 (23)	−0.44	0.344 (31)	−0.43
$B_0 - B_{16}$ (MHz)	1.530827 (74)	1.99	1.5092 (23)	1.94
$C_0 - C_{16}$ (MHz)	0.842223 (66)	1.04	0.822875 (96)	1.02
Δ_i (uÅ^2)	0.005690 (30)	0.0017	−0.00007 (62)	−0.0041
	ν_{22}			
$A_0 - A_{22}$ (MHz)	1.504 (55)	1.69		
$B_0 - B_{22}$ (MHz)	0.0042 (46)	0.12		
$C_0 - C_{22}$ (MHz)	−0.682660 (84)	−0.67		
Δ_i (uÅ^2)	−0.1840 (11)	−0.195		
	ν_{15}			
$A_0 - A_{15}$ (MHz)	−0.66 (23)	0.60		
$B_0 - B_{15}$ (MHz)	0.342 (19)	0.20		
$C_0 - C_{15}$ (MHz)	0.82723 (12)	0.94		
Δ_i (uÅ^2)	0.2324 (47)	0.293		

stants had to be fixed beyond the first quantum, precluding meaningful analysis, although fixing these values to their linearly predicted values resulted in satisfactory least-squares fits, suggesting that these are reasonable estimates of their real values.

3.3. [^{35}Cl]-Chloropyrazine, ν_{17} (v = 1, 2)

The second lowest-energy fundamental of [^{35}Cl]-chloropyrazine, ν_{17} (A′, 309 cm^{-1}), is an in-plane bending mode of the chlorine atom relative to the aryl ring. The final least-squares fit of ν_{17} to a sextic distorted-rotor Hamiltonian contained 2169 independent transitions. The sextic distortion terms (Φ_J, Φ_K, ϕ_J) that could not be satisfactorily determined were fixed to their ground-state values. As with ν_{24}, the computed vibration-rotation interaction constants provided excellent initial predictions of the rotational constants; the largest magnitude discrepancy (0.86 MHz, 3.4%) occurs again with $A_0 - A_{17}$. The overtone $2\nu_{17}$ (A′, 618 cm^{-1}) was very well-predicted by an extrapolation from the ground state and ν_{17} constants. It is predicted to be nearly degenerate with the experimental frequency of fundamental ν_{15} (A′, 618 cm^{-1}) with possible Fermi and Coriolis coupling. Additionally, $\nu_{24} + \nu_{16}$ (A″, 623 cm^{-1}) is predicted to be only a few wavenumbers higher in energy, creating a potential triad of coupled states. Due to its low intensity, possible coupling to nearby states, and the spectral density, only 265 transitions were incorporated into the final least-squares fit. A sextic distorted-rotor Hamiltonian was employed with sextic and the purely K-dependent quartic centrifugal distortion terms fixed to values extrapolated from the corresponding values of the ground state and ν_{17}.

Fig. 7 illustrates an analysis similar to that in Fig. 6, but for the ν_{17} series. The smooth change from ground vibrational state to successive quanta of ν_{17} of the rotational constants (Fig. 7a) and inertial defect values (Fig. 7b) validates each of these determined constants. The quartic distortion constants (Fig. 7c) show purely J-dependent terms that are highly similar to the ground state values, while the purely K-dependent terms varied most from ground state to first quantum and had to be fixed for the second quantum. Nevertheless, the smooth progression of those constants that were fit for all three states and the satisfactory least-squares fits where the terms had to be fixed suggest that the experimentally determined values are reasonably well determined and free of perturbation. Four sextic distortion terms (Fig. 7d) were determined for ν_{17} and had to be fixed to the extrapolated values for $2\nu_{17}$; the value of δ_J was fixed to the ground state value for both vibrational states, which appears reasonable based on the trend of similarity between ground state and purely J-dependent distortion terms.

3.4. [^{35}Cl]-Chloropyrazine, ν_{23} and ν_{16}

The fourth and fifth lowest-energy vibrationally excited states are ν_{23} (A″, 413 cm^{-1}) and ν_{16} (A′, 435 cm^{-1}). Fundamental ν_{23} is

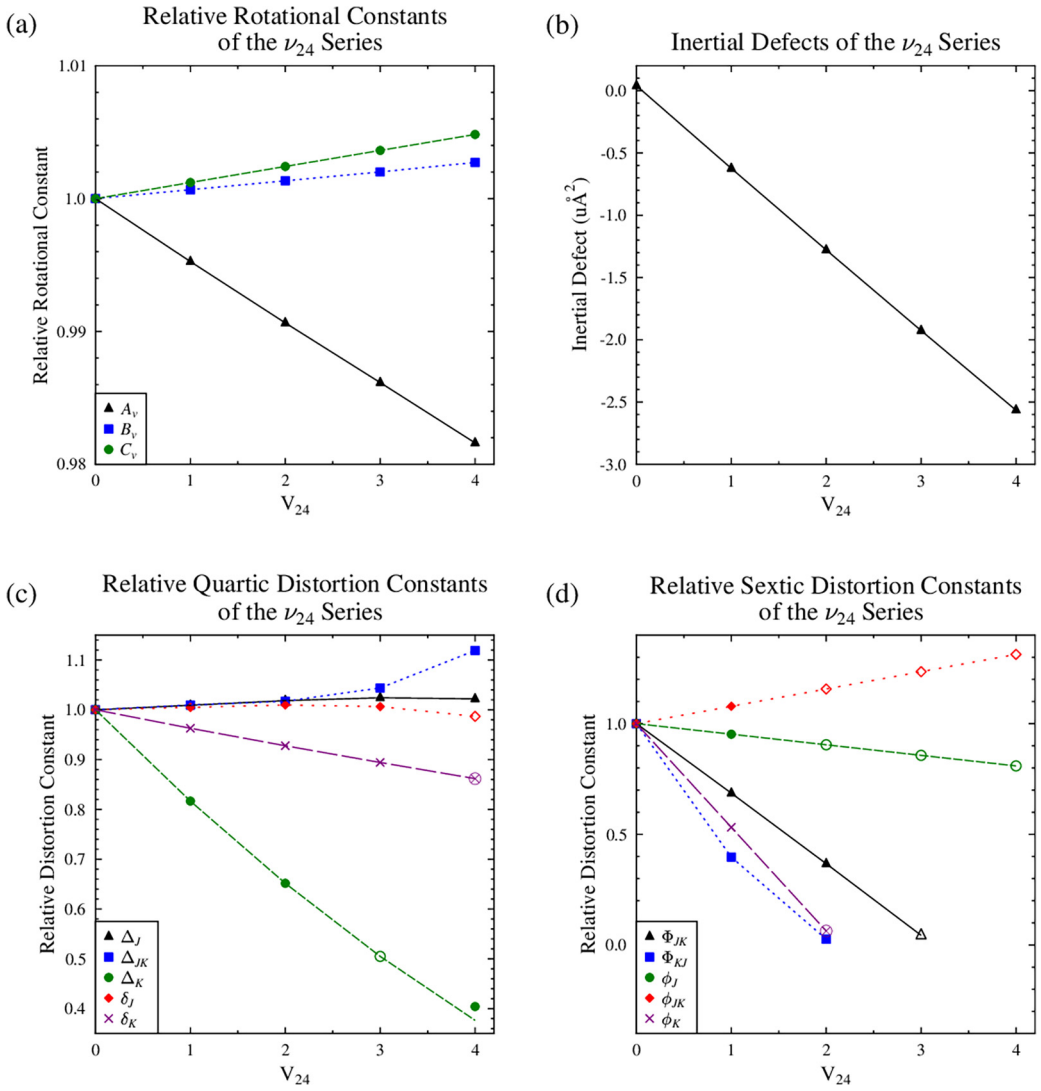

Fig. 6. (a) Relative rotational constants, (b) inertial defect, (c) relative quartic centrifugal distortion, and (d) relative sextic centrifugal distortion constants for [^{35}Cl]-chloropyrazine as a function of vibrational excitation (v_{24} = 0, 1, 2, 3, 4). The trendline for each series is a polynomial fit of all corresponding constants included in their least-squares fits. Open symbols represent values fixed in their least-squares fits to those extrapolated from the lower-energy states in the vibrational sequence.

an A″ ring deformation mode in which C-3 and C-6 (as labeled in Fig. 1) have large amplitude motions and C-l and C-4 are nearly stationary. Fundamental ν_{16} is an A′ mode predominantly characterized by a σ_{C-Cl} stretching motion. The transitions of the higher energy ν_{16} are easily identified, assigned, and least-squares fit using the experimental ground state rotational constants (Table 3) with predicted vibration-rotation interaction constants (Table 2). The final least-squares fit of ν_{16} (Table 3) included 1312 transitions and resulted in a sextic distorted-rotor Hamiltonian with all sextic terms fixed to their ground state values. The value of $A_0 - A_{16}$, which was predicted at −0.44 MHz, was measured to be +0.3721 MHz (Table 4). While the error in the predicted A_{16} value versus the experimentally observed A_{16} value is relatively small compared to the magnitude of A_{16} (0.013%), it has the wrong predicted sign. As will be discussed further below, this difference is most likely due to the computational modeling of this vibrational mode. The vibration-rotation interaction constants corresponding to B_{16} and C_{16} were well-predicted by B3LYP.

In contrast, the lower energy ν_{23} (A″, 413 cm^{-1}) was significantly more challenging to identify than ν_{16}, despite having slightly more intense transitions, due to having rotational constants very similar to two other near-energy vibrationally excited states ν_{22} (A″, 477 cm^{-1}) and $\nu_{24} + \nu_{17}$ (A″, 497 cm^{-1}). As shown in Table 3, the rotational constants of these three states vary at most by 3.1, 1.1, and 0.10 MHz for A_v, B_v, and C_v, respectively. With only *a*-type transitions available in any of these data sets, the values of B_v and C_v are the most precisely measured and most reliable for assigning the vibrational states. As the K_a = 0,1 oblate-degenerate series are the most intense for each state and highly dependent on C_v, the very close values of C_v made the initial assignment challenging with all three states predicted to have transitions in the same region separated from transitions in other bands by approximately the value of 2*C*. When the final least-squares fits were completed, the assignment of ν_{22} (A″, 477 cm^{-1}) was made using its predicted vibration–rotation interaction constants, particularly its 1.504 MHz experimental value of $A_0 - A_{22}$ (predicted 1.69 MHz) compared to the larger ones predicted for $A_0 - A_{23}$ (predicted 4.45 MHz) or $A_0 - A_{24,17}$ (3.23 MHz extrapolated from ground state, ν_{24}, and ν_{17}). Differentiating ν_{23} from $\nu_{24} + \nu_{17}$ remained a challenge based upon the rotational constants alone, where all three rotational constants are remarkably similar. The assignment of each of these states was based upon intensity analysis and the number of transitions observed and least-squares fit to a distorted-rotor Hamiltonian. For greater than twenty pairs of

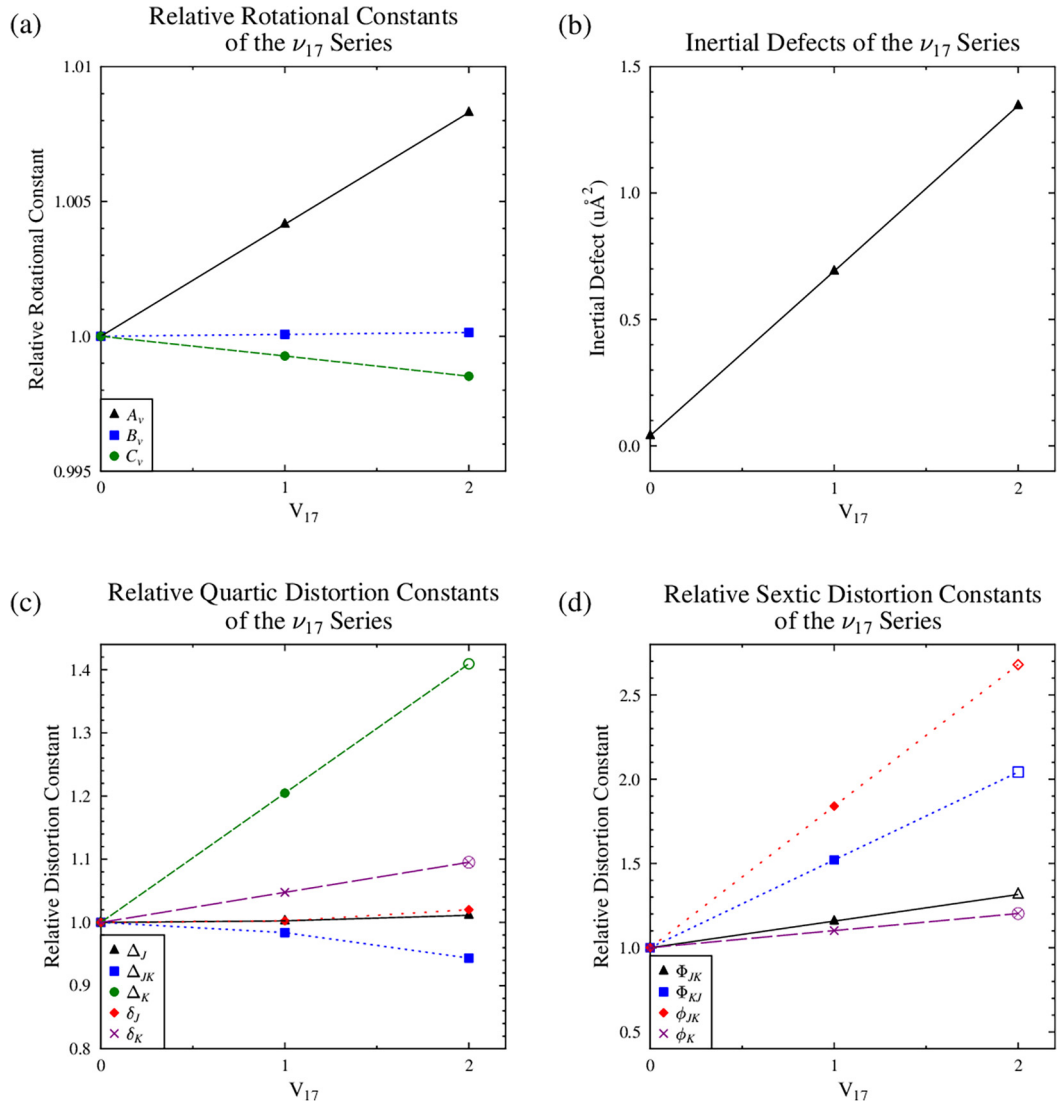

Fig. 7. (a) Relative rotational constants, (b) inertial defect, (c) quartic centrifugal distortion, and (d) sextic centrifugal distortion constants for [^{35}Cl]-chloropyrazine as a function of vibrational excitation (v_{17} = 0, 1, 2). The trendline for each series is a polynomial fit of all corresponding constants included in their least-squares fits. Open symbols represent values fixed in their least-squares fits to those extrapolated from the lower-energy states in the vibrational sequence.

transitions with identical quantum numbers assigned to each state, the intensity was universally greater for one than the other. The more intense state was assigned to ν_{23}, the less intense state assigned to $\nu_{24} + \nu_{17}$. Satisfyingly, these vibrational state assignments also matched the experimental rotational constants to the predicted rotational constants most closely. A final piece of evidence supports these assignments: the number of measured transitions. The number of transitions assigned and least-squares fit to ν_{23} was 1672, which is more than the 1312 assigned and least-squares fit to the higher energy ν_{16} and much more than for ν_{22} and $\nu_{24} + \nu_{17}$ (401 and 341 transitions, respectively). As the energy of the state increases, the number of observable transitions decreases; this behavior is partially responsible for a decrease in the number of constants that can be satisfactorily determined in least-squares fitting. A sextic distorted-rotor Hamiltonian with Φ_{JK} allowed to vary was used for ν_{23} with all other sextic terms fixed to ground state values; all sextic terms and Δ_K are fixed for $\nu_{24} + \nu_{17}$ (Table 3).

While satisfactory single-state least squares fits were obtained for ν_{23} and ν_{16}, they are predicted to have small *a*-type and *b*-type Coriolis interactions. Computed values of the Coriolis coefficients are $|\zeta^a_{23,16}|$ = 0.0118 and $|\zeta^b_{23,16}|$ = 0.0276 (B3LYP/6-311+G (2d,p)). Using Eq. (1) (and the analogous relation for G_b) [17], these ζ values result in rather small predicted coupling terms ($|G_a|$ = 143 MHz and $|G_b|$ = 91.8 MHz) given the measured vibrational frequencies [9] and the experimental rotational constants.

$$G_a = \frac{\omega_{23} + \omega_{16}}{\sqrt{\omega_{23} \times \omega_{16}}} \zeta^a_{23,16} A \approx 2\zeta^a_{23,16} A \quad (1)$$

As a result of the spectral density and small perturbation between states, a coupled fit was not obtained and many transitions for each of the two states could be easily fit to single-state models that resulted in centrifugal distortion constants without obvious signs of perturbation. Furthermore, it is interesting to note that there is no evidence of an inverse relationship between the effective experimental $A_0 - A_v$ values (0.12 MHz and 0.81 MHz for ν_{23} and ν_{16}, respectively; Table 4), which would be expected if the states were exhibiting *a*-type Coriolis perturbation.

3.5. [^{35}Cl]-Chloropyrazine, ν_{22} and $\nu_{24} + \nu_{17}$

The sixth lowest-energy vibrationally excited state is ν_{22} (A″, 477 cm^{-1}), an out-of-plane ring deformation mode in which the chlorine atom is nearly stationary. The seventh vibrationally

excited state is the simple combination of the two lowest-energy fundamentals $\nu_{24} + \nu_{17}$ (A″, 497 cm^{-1}). Satisfactory least-squares fits were obtained for each of these states and their assignments made based upon a combination of their line intensities and vibration-rotation interaction constants. Each of these states was fit to a sextic distorted-rotor Hamiltonian with sextic and Δ_K terms fixed to ground state (ν_{22}) or extrapolated ($\nu_{24} + \nu_{17}$) values as necessary (Table 3), except Φ_J and Φ_K, which were fixed to the ground state computed values as they were not determined for any of the vibrational states. These states were the first ones in which Δ_K could not be determined due to the limited data sets (401 transitions for ν_{22} and 341 transitions for $\nu_{24} + \nu_{17}$). This is not surprising due to the strong dependence of Δ_K on K, its high correlation to A_v, and the limited number of only a-type transitions. There is a dramatic drop-off in the number of transitions that can be measured, assigned, and included in the least-squares fits of these states. While this is partially due to the spectral density and lines obscured by or shifted by accidentally overlapping transitions of other vibrational states, there is the likelihood that these vibrational states are impacted by Coriolis or Fermi coupling. Notably, $3\nu_{24}$, which is predicted to be about two thirds as intense as the two states in question has over 600 transitions included in its final least-squares fit. Despite the possibility of perturbations due to the coupling of these states, the experimental rotational constants and quartic centrifugal distortion constants determined in these single state fits show reasonable agreement with the computational predictions (Table 4) and those extrapolated from the ground state.

3.6. [^{35}Cl]-Chloropyrazine, $\nu_{24} + \nu_{23}$, ν_{15}, and $\nu_{24} + \nu_{16}$

The 8th – 12th lowest-energy vibrationally excited states are $3\nu_{24}$ (A″, 564 cm^{-1}), $\nu_{24} + \nu_{23}$ (A″, 601 cm^{-1}), ν_{15} (A″, 618 cm^{-1}), $2\nu_{17}$ (A′, 618 cm^{-1}), and $\nu_{24} + \nu_{16}$ (A″, 623 cm^{-1}), of which overtones $2\nu_{17}$ and $3\nu_{24}$ have previously been discussed. Fundamental ν_{15} (A″, 618 cm^{-1}) is an in-plane ring deformation mode and the highest-energy fundamental observed and least-squares fit in the current work. While each of these states is also well fit to a single-state model (Table 3), it is certain that these are effective fits and that these states would be better treated by a multi-state fit including Coriolis and Fermi coupling terms. For each of these states, which include between 120 and 300 transitions, extrapolated or ground-state sextic constants were fixed and a sextic Hamiltonian least-squares fit was obtained. The experimental vibration-rotation interaction constants for ν_{15} were, once again, in excellent agreement with the computational predictions for $B_0 - B_{15}$ and $C_0 - C_{15}$ (Table 4). The experimental value of $A_0 - A_{15}$ is −0.66 (23) MHz with a predicted value of 0.60 MHz. This large difference may be due, in part, to the poor determination of A_v from a very small data set of 154 transitions. Given the quality of the predicted vibration–rotation interaction constants for other states, it is very likely that the apparent value of A_{15} is impacted by the unaddressed coupling with the near-energy vibrational states.

3.7. [^{35}Cl]-Chloropyrazine, $\nu_{24} + \nu_{22}$, $2\nu_{24} + \nu_{17}$, $\nu_{17} + \nu_{23}$, and $\nu_{16} + \nu_{17}$

The 13th – 16th lowest-energy vibrationally excited states are four combination states, $\nu_{24} + \nu_{22}$ (A′, 665 cm^{-1}), $2\nu_{24} + \nu_{17}$ (A′, 685 cm^{-1}), $\nu_{17} + \nu_{23}$ (A″, 722 cm^{-1}), and $\nu_{16} + \nu_{17}$ (A′, 601 cm^{-1}). All of these states were well-predicted by extrapolation from ground state and the appropriate lower-energy excited state spectroscopic constants. All of these combination states were fit to sextic Hamiltonians (Table 3), which resulted in well-determined rotational constants. All quartic and sextic centrifugal distortion constants that could not be determined satisfactorily were fixed to extrapolated constants. Notably, 723 independent transitions were measured for $2\nu_{24} + \nu_{17}$, which highlights that this state has transitions with fewer accidental overlaps and displays less impact of perturbation than its near-energy neighbors at low K_a. This is the highest-energy state for which a sextic distorted rotor Hamiltonian least-squares fit was achieved.

3.8. [^{37}Cl]-Chloropyrazine, ground state

As with the [^{35}Cl]-isotopologue, the combination of previous rotational data [7,8] and computed distortion constants resulted in a convenient initial prediction of the low K_a series. At natural abundance, ^{37}Cl (~25%) is approximately one third as abundant as ^{35}Cl (~75%). As a result of the reduced intensity, a smaller number of transitions (N_{lines} = 2694) were included in the least-squares fit of the [^{37}Cl]-chloropyrazine ground vibrational state. At lower relative intensity, transitions of [^{37}Cl]-chloropyrazine are more influenced by accidental overlaps with transitions of the [^{35}Cl]-isotopologue and the latter's lower-energy vibrational states. The final data set of ground state [^{37}Cl]-chloropyrazine allowed for a sextic distorted-rotor Hamiltonian with all terms except Φ_J and Φ_K employed (Table 5). As with the [^{35}Cl]-isotopologue, Φ_J and Φ_K were fixed to their computed values. The predicted values for all quartic distortion constants were in reasonable agreement with their experimental values. The sextic constants are in weaker agreement between the computed and experimental values, particularly ϕ_J and ϕ_{JK}. The computed value for ϕ_{JK} exhibits a discrepancy of approximately 220%, compared to the experimental value, which is similar to the situation described for the [^{35}Cl]-isotopologue. The experimentally determined values of ϕ_{JK} for the isotopologues, however, were fairly similar (2.40×10^{-11} MHz for [^{35}Cl]- and 1.97×10^{-11} MHz for [^{37}Cl]-chloropyrazine ground vibrational states) and, thus the constant was included in the final least-squares fit for [^{37}Cl]-chloropyrazine, as well. The original estimates of $A_0^{(A)}$, $B_0^{(A)}$ and $C_0^{(A)}$ [7,8], were in reasonable agreement with the improved constants determined in this work, and in fact, the previous value of $A_0^{(A)}$ is within its quoted error bars (Table 1, column 3) from the value of $A_0^{(A)}$ determined in the current work. As expected due to the proximity of the chlorine atom to the a-axis, the $^{35/37}$Cl-isotopic substitution results in a very small change in $A_0^{(A)}$ (0.0985 (37) MHz). Much larger changes are observed for $B_0^{(A)}$ (47.50579 (13) MHz) and $C_0^{(A)}$ (29.38557 (12) MHz) due to the large distance of the chlorine atom from those axes. Unfortunately, a precise structure determination of chloropyrazine is not possible using the current spectral data. Due to high spectral density, nitrogen and carbon isotopologues cannot be discerned in natural abundance. Structure determination of this species would require intentional isotopic substitution of the hydrogen, nitrogen, and carbon atoms.

3.9. [^{37}Cl]-Chloropyrazine, ν_{24} (v = 1, 2)

As with the [^{35}Cl]-isotopologue, the ν_{24} series was observable, though only for ν_{24} = 0, 1, 2 due to the lower isotopic abundance. A total of 1943 and 1155 independent transitions were included in the final least-squares fits for ν_{24} and $2\nu_{24}$, respectively. Transitions for both of these excited states were treated with an A-reduction sextic distorted-rotor Hamiltonian; all distortion terms that could not be fit were fixed to ground vibrational state or extrapolated values, as necessary (Table 5). The computed vibration-rotation interaction constants combined with the experimental ground state rotational constants provided a very satisfactory prediction of the low K_a series. The predicted vibration-rotation interaction values were in approximately the same agreement seen for the [^{35}Cl]-isotopologue (Table 4). As shown in Fig. 8, the resulting rotational constants (Fig. 8a), inertial defects (Fig. 8b), and distortion constants (Fig. 8c and d) vary smoothly across the vibrational excitation series. Once again, purely K-dependent dis-

Table 5
Spectroscopic constants for [^{37}Cl]-chloropyrazine and its vibrationally excited states (A-reduced Hamiltonian, I^r representation).

	B3LYP/6-311+(2d,p) [^{37}Cl] G.S.	Current work [a] [^{37}Cl] G.S.	ν_{24} [b] A″, 188 cm^{-1}	ν_{17} [b] A′, 309 cm^{-1}	$2\nu_{24}$ A′, 376 cm^{-1}
$A_v^{(A)}$ (MHz)	6065	6041.9335 (18)	6013.0747 (23)	6067.2616 (34)	5985.0199 (20)
$B_v^{(A)}$ (MHz)	1592	1616.596220 (63)	1617.695202 (78)	1616.704444 (89)	1618.792426 (69)
$C_v^{(A)}$ (MHz)	1261	1275.226233 (58)	1276.769339 (71)	1274.294069 (75)	1278.306619 (45)
Δ_J (kHz)	0.0649	0.0641439 (13)	0.0647277 (17)	0.0643154 (28)	0.0653349 (24)
Δ_{JK} (kHz)	0.323	0.324112 (32)	0.327302 (58)	0.319677 (96)	0.329639 (86)
Δ_K (kHz)	1.05	1.0694 (27)	0.8680 (36)	1.2818 (47)	0.7013 (30)
δ_J (kHz)	0.0148	0.0148832 (21)	0.0149550 (27)	0.0149239 (30)	0.0150302 (11)
δ_K (kHz)	0.340	0.33857 (12)	0.32604 (16)	0.35539 (20)	0.314474 (83)
Φ_J (Hz)	0.000000114	[0.0000001139][c]	[0.0000001139][c,d]	[0.0000001139][c,d]	[0.0000001139][c,d]
Φ_{JK} (Hz)	0.000134	0.0001335 (98)	0.000113 (13)	0.000225 (16)	0.0000896 (54)
Φ_{KJ} (Hz)	−0.000592	−0.000666 (35)	−0.000360 (56)	[−0.0006663][d]	[−0.00005469][e]
Φ_K (Hz)	0.00114	[0.001144][c]	[0.001144][c,d]	[0.001144][c,d]	[0.001144][c,d]
φ_J (Hz)	0.000000649	0.000000516 (65)	0.000000540 (85)	0.000000493 (93)	[0.0000005649][e]
φ_{JK} (Hz)	0.0000632	0.0000197 (44)	0.0000278 (60)	0.0000585 (78)	[0.00003605][e]
φ_K (Hz)	0.00195	0.00175 (17)	0.00141 (24)	0.00280 (28)	[0.001071][e]
N_{lines}		2694	1943	1427	1155
σ		0.039	0.043	0.042	0.043
Δ_i (uÅ^2)	0.055	0.040934 (33)	−0.627106 (56)	0.700945 (55)	−1.28342 (34)
κ	−0.862	−0.857	−0.856	−0.857	−0.855
X_{aa} Cl (MHz)	−54.1				
X_{bb} Cl (MHz)	22.9				
X_{cc} Cl (MHz)	31.2				

	ν_{23} [b] A″, 413 cm^{-1}	ν_{16} [b] A′, 435 cm^{-1}
$A_v^{(A)}$ (MHz)	6037.3498 (62)	6041.589 (31)
$B_v^{(A)}$ (MHz)	1616.75950 (25)	1615.0870 (23)
$C_v^{(A)}$ (MHz)	1275.941846 (71)	1274.403358 (76)
Δ_J (kHz)	0.064336 (20)	0.06428 (21)
Δ_{JK} (kHz)	0.32353 (30)	0.341 (11)
Δ_K (kHz)	1.084 (16)	[1.0694][d]
δ_J (kHz)	0.014918 (10)	0.01484 (11)
δ_K (kHz)	0.33741 (38)	0.3437 (31)
Φ_J (Hz)	[0.0000001139][c,d]	[0.0000001139][c,d]
Φ_{JK} (Hz)	0.000135 (28)	[0.0001336]
Φ_{KJ} (Hz)	[−0.0006663][d]	[−0.0006663][d]
Φ_K (Hz)	[0.001144][c,d]	[0.001144][c,d]
φ_J (Hz)	[0.0000005162][d]	[0.0000005162][d]
φ_{JK} (Hz)	[0.00001971][d]	[0.00001971][d]
φ_K (Hz)	[0.001758][d]	[0.001758][d]
N_{lines}	341	183
σ	0.041	0.040
Δ_i (uÅ^2)	−0.21327 (10)	−0.00007 (62)
κ	−0.847	−0.857

[a] Least-squares fit including newly measured transitions and data from Refs. [7,8].
[b] Fundamental vibrational frequencies from Ref. [9].
[c] Value fixed to B3LYP/6-311+G(2d,p) computed value.
[d] Value fixed to ground state value.
[e] Value fixed based upon extrapolation from other vibrational states in its corresponding series.

tortion constants varied most between quanta of ν_{24}, while purely *J*-dependent constants remained most similar to those of the ground state.

3.10. [^{37}Cl]-Chloropyrazine, ν_{17}, ν_{23}, and ν_{16}

Transitions of three additional [^{37}Cl]-chloropyrazine fundamentals ν_{17}, ν_{23}, and ν_{16} were measured and least-squares fit using sextic distorted-rotor Hamiltonian models. Any sextic or quartic centrifugal distortion constants that could not be satisfactorily determined were fixed to their corresponding [^{37}Cl]-chloropyrazine ground-state values. Once again, observation and assignments of these fundamentals was facilitated by employing the ground state distortion constants and the computed vibration-rotation interaction constants (Table 4). Each of the predicted vibration-rotation interaction values is in reasonable agreement with the experimentally-determined values. The greatest difference between the observed and calculated values occurs for ν_{16}, where $A_0 - A_{16}$ is 0.344 MHz and predicted to be −0.43 MHz. Since the value of A_{16} was determined to three decimal places and ν_{16} for the [^{35}Cl]-isotopologue displays nearly the same discrepancy in sign and magnitude, it is not likely due to the small number of transitions (N_{lines} = 183) available, and this issue will be discussed in further detail below.

4. Discussion and conclusions

This work establishes that the centrifugal distortion contants and vibration-rotation interaction constants obtained from the

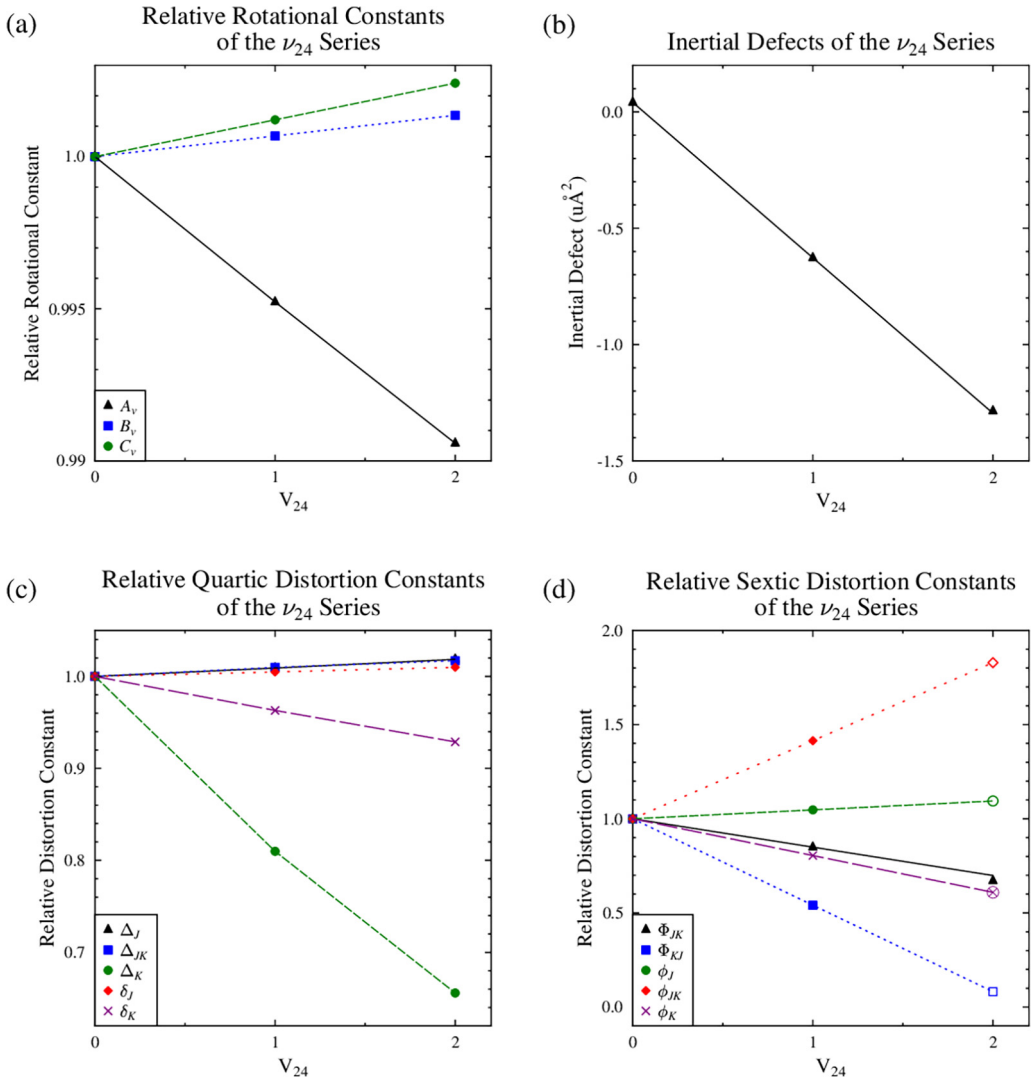

Fig. 8. (a) Relative rotational constants, (b) inertial defect, c) quartic centrifugal distortion, and d) sextic centrifugal distortion constants for [^{37}Cl]-chloropyrazine as a function of vibrational excitation (v_{24} = 0, 1, 2). The trendline for each series is a polynomial fit of all corresponding constants included in their least-squares fits. Open symbols represent points fixed to their extrapolated values in their least-squares fits.

B3LYP/6-311+(2d,p) optimization and anharmonic frequency calculation are of sufficiently high-quality to be of great value in the analysis of experimental spectra. Although the computed values do not fall within the estimated uncertainty of the experimental values, they are nevertheless of great utility for their ability to make initial predictions of the spectra. Given the high quality of the experimental data, the small differences between the experimental and computed values of the quartic centrifugal distortion constants for the ground state are almost solely due to error in the computational geometry and force constants. The differences between the experimental and computed sextic distortion constants, however, are much larger. Discrepancies are as large as 11% for the on-diagonal terms and 220% for the off-diagonal terms. These larger differences in the sextic terms are due to a combination of higher errors in computational prediction, the relatively less accurate determination of all of the sextic terms compared to the quartic terms, and the fact that Φ_J and Φ_K had to be fixed to the computationally predicted value for both isotopologues. It can be seen that throughout the analysis of vibrational excited states in this work, we have employed the strategy of using sextic Hamiltonians and using ground-state or computed values for any constants that could not be least-squares fit. This technique is partially enabled by the relatively recent ability to computationally predict sextic distortion constants. When distortion terms that cannot be determined are instead fixed to zero, other constants in the least-squares fit shift in unrealistic ways to compensate for the zeroed constants' absence. By fixing undeterminable constants to the ground-state or predicted values, the set of determined constants show greater consistency and appear more physically meaningful.

As mentioned previously, initial estimates of the spectroscopic constants for combination states were linearly extrapolated using the experimentally determined ground vibrational state and corresponding fundamental state constants. This procedure proved quite successful. Because of the unusually large number of combination states analyzed in this work, our results provide a useful calibration of the quantitative accuracy of this procedure and demonstrate that it can be very effective. Table 6 provides the rotational and quartic distortion constants, along with differences (*obs.* – *calc.*) between these and the extrapolated values, for the observed combination states of [^{35}Cl]-chloropyrazine. The *obs.* – *calc.* values are generally quite small for the both the rotational and quartic distortion constants. It is unlikely that transitions for most of these combination states would have been assigned correctly and least-squares fit without the extrapolated values. The extrapolated values for overtone and combination states are of such utility that it becomes easier to assign the spectra of overtone

and combination states than fundamentals with high energies. The rotational constants obtained for combination and overtone states obtained by extrapolation from lower-energy states are comparable in accuracy to those obtained for fundamental states by using computed vibration-rotation interaction constants. The extrapolated quartic distortion constants, however, are substantially more effective for making predictions of combination and overtone spectra than the ground-state distortion constants are for fundamental states. This is evident in the least-squares fitting of $4\nu_{24}$, where 266 independent transitions were identified and least-squares fit. Fundamentals ν_{21} and ν_{14} were not identified or least-squares fit in this work, despite having roughly the same expected intensity as $4\nu_{24}$. This demonstrates that the prediction of the distortion constant changes by extrapolation provides a distinct advantage in identifying the relatively low intensity spectra of higher energy states in comparison to fundamental states, where no such predictions are available. (Note that by design, the effective fits obtained for each of these states excluded all high error transitions and used fixed values of all distortion constants that varied substantially from their extrapolated values. This constrained each of these least squares fits to obtain rotational and distortion constants that are relatively free of the effects of coupling between states.)

The isotopic changes in the rotational and distortion constants for chloropyrazine are very similar to those observed in chlorobenzene [2], 4-chloropyridine [3], and 2-chloropyrimidine [6], as shown in Table 7. Because the principal axis coordinates of the chlorine atom are expected to be very similar between all four molecules, it is not surprising that the rotational constant shifts are also very similar, as would be predicted by Kraitchman's equations [18]. The shifts in A_e are either zero (for C_{2v} molecules) or near-zero, since the b coordinate is zero (for C_{2v} molecules) or very small (~0.02 Å in chloropyrazine), while the shifts in A_0 are harder to predict because of the effects of vibration-rotation interactions, but are still expected to be quite small. The shifts in B_0 or C_0 are primarily related to the a coordinate of the chlorine atom, which is much larger and rather similar in all four molecules. Less predictable is that the isotopic changes in the quartic centrifugal distortion constants are also very similar. These range from 1.2 to 6.3% for both chloropyrazine and chlorobenzene, with the largest changes observed in the purely J-dependent terms and the smallest changes in the purely K-dependent terms.

The comparison of the experimental $A_0 - A_v$, $B_0 - B_v$, $C_0 - C_v$ values between [^{35}Cl]- and [^{37}Cl]-isotopologues of chloropyrazine (Table 4) exhibits a very close agreement for every vibrational state in both the experimental and computed values. The fact that the experimental isotopic changes in the vibration-rotation interaction constants (ranging from 0.0021 to 0.225 MHz) are as small as they are predicted to be provides welcome confirmation of the spectral assignment and the accuracy of the experimental rotational constants of each state. With the exceptions of $A_0 - A_{16}$ and $A_0 - A_{15}$, there is also very close agreement between the experimental vibration-rotation interaction constant values and their calculated values. These differences in the $A_0 - A_{16}$ values do not appear to be due to either the errors in the experimental determination of the rotational constants or due to the unaddressed Coriolis coupling with ν_{23} (see above). They are likely due to the error in the computational value of $A_0 - A_{16}$, which, given the small magnitude of those values (experimental and computed), are difficult to predict. Fundamental ν_{16} is an in-plane ring deformation mode with a substantial σ_{C-Cl} stretch contribution. Vibration-rotation interaction constants for fundamentals ν_{17}, ν_{24}, ν_{23} are all computationally well predicted and involve either large motions of the chlorine atom or out-of-plane motions of the ring atoms. Thus, it is unlikely that the computed geometry is responsible for the differences in computed

Table 6
Experimentally determined spectroscopic constants and differences from linearly extrapolated predictions for combination states of [^{35}Cl]-chloropyrazine (A-reduced Hamiltonian, I^r representation).

	$\nu_{24}+\nu_{17}$ A″, 497 cm^{-1}	*obs. – calc.*	$\nu_{24}+\nu_{23}$ A′, 601 cm^{-1}	*obs. – calc.*	$\nu_{24}+\nu_{16}$ A″, 623 cm^{-1}	*obs. – calc.*	$\nu_{24}+\nu_{22}$ A′, 665 cm^{-1}	*obs. – calc.*
$A_v^{(A)}$ (MHz)	6038.800 (58)	0.30	6006.61 (58)	−2.21	6010.96 (13)	−2.06	6011.69 (40)	−0.20
$B_v^{(A)}$ (MHz)	1665.1593 (48)	−0.18	1666.554 (46)	1.17	1663.757 (11)	0.069	1665.233 (32)	0.019
$C_v^{(A)}$ (MHz)	1305.248771 (67)	0.0083	1306.83008 (10)	−0.10	1305.36512 (13)	0.013	1306.87357 (11)	−0.0039
Δ_J (kHz)	0.06850 (37)	0.00068	0.06814 (61)	0.00031	0.06607 (42)	−0.0021	0.06453 (49)	−0.0014
Δ_{JK} (kHz)	0.308 (15)	−0.025	0.318 (18)	−0.019	0.405 (13)	0.069	0.461 (15)	0.045
Δ_K (kHz)	[1.079]		[0.8669]		[0.8358]		[0.8632]	
δ_J (kHz)	0.01638 (18)	0.00038	0.01597 (30)	−0.000014	0.01504 (20)	−0.0011	0.01427 (24)	−0.00070
δ_K (kHz)	0.3534 (28)	0.0010	[0.3348]		[0.3350]		[0.3454]	
N_{lines}	341		122		182		127	
σ	0.043		0.048		0.048		0.044	
Δ_i (uÅ^2)	−0.0008 (12)		−0.664 (12)		−0.6787 (27)		−0.8461 (80)	
κ	−0.848		−0.847		−0.848		−0.848	
	$2\nu_{24}+\nu_{17}$ A′, 685 cm^{-1}	*obs. – calc.*	$\nu_{17}+\nu_{23}$ A″, 722 cm^{-1}	*obs. – calc.*	$\nu_{17}+\nu_{16}$ A′, 744 cm^{-1}	*obs. – calc.*		
$A_v^{(A)}$ (MHz)	6009.7379 (25)	−0.65	6062.5865 (81)	0.021	[6066.77]			
$B_v^{(A)}$ (MHz)	1665.355081 (90)	−1.01	1664.39765 (24)	0.019	1662.5775 (40)	−0.11		
$C_v^{(A)}$ (MHz)	1306.881873 (61)	0.056	1304.406075 (86)	0.0084	1302.75937 (14)	−0.056		
Δ_J (kHz)	0.0679251 (58)	−0.00086	0.0673954 (42)	0.0000020	0.0677816 (49)	0.0000081		
Δ_{JK} (kHz)	0.334050 (94)	0.011	0.33059 (64)	0.0014	[0.3281]			
Δ_K (kHz)	0.9407 (66)	0.045	1.260 (31)	−0.016	[1.246]			
δ_J (kHz)	0.0159618 (30)	−0.00031	[0.01595]		[0.01609]			
δ_K (kHz)	0.33733 (15)	−0.0030	[0.3643]		[0.3645]			
N_{lines}	723		136		28			
σ	0.042		0.042		0.041			
Δ_i (uÅ^2)	−0.853612 (43)		0.43886 (12)		0.654 (14)			
κ	−0.848		−0.849		−0.849			

Table 7
Comparison of experimental spectroscopic constants for [^{35}Cl]- and [^{37}Cl]-chloroarenes.[a]

	chloropyrazine		chlorobenzene [2]		4-chloropyridine [3]		2-chloropyrimidine [6]	
	Δ^b	% change	Δ^b	% change	Δ^b	% change	Δ^b	% change
A_0 (MHz)	0.0985 (23)	0.002	−0.0016 (52)	−0.00003	−0.1 (8)	−0.002	−0.037 (31)	−0.0006
B_0 (MHz)	47.505785 (82)	2.9	43.997986 (72)	2.8	44.421 (5)	2.8	48.277 (2)	2.8
C_0 (MHz)	29.385572 (76)	2.3	27.100040 (69)	2.2	28.089 (6)	2.3	29.6237 (8)	2.2
Δ_J (kHz)	0.0029044 (16)	4.3	0.0025896 (62)	4.3				
Δ_{JK} (kHz)	0.010735 (35)	3.2	0.008182 (97)	2.9				
Δ_K (kHz)	−0.0125 (34)	−1.2	−0.0091 (93)	−1.0				
δ_J (kHz)	0.0009985 (28)	6.3	0.0008981 (27)	6.2				
δ_K (kHz)	0.01013 (15)	2.9	0.00905 (27)	2.9				

[a] Experimental spectroscopic constants for all chloroarenes are provided in Tables S1–S4 of the Supplementary Material.
[b] Δ = [^{35}Cl]-isotopologue value − [^{37}Cl]-isotopologue value.

and experimental constants. It would generally be expected that the cubic force constants required to predict the vibration-rotation interaction constants would be more difficult to predict accurately than the structural parameters and thus more likely contribute to the observed discrepancy in $A_0 - A_{16}$. The similar situation of ν_{15} is more difficult to evaluate, but could be due to similar issues.

An interesting comparison can be made between the vibration-rotation interaction constants for [^{35}Cl]-chloropyrazine and [^{35}Cl]-2-chloropyrimidine for which the rotational spectra of four fundamentals have been reported [6]. Table 8 shows vibration-rotation interaction values for the corresponding vibrationally excited states for each species. The assignments of the fundamental modes of [^{35}Cl]-2-chloropyrimidine were not made in the previous work. Definitive assignment is now possible using computationally predicted vibration-rotation interaction constants, thus allowing the new assignments presented in Table 8. The lowest-energy vibration state (ν_{16}, B_1) is an out-of-plane ring deformation mode involving significant chlorine atom motion. Its overtone, $2\nu_{16}$, was also reported and assigned. The second lowest energy mode (ν_{24}, B_2) is the in-plane bend of $\sigma_{C\text{-}Cl}$. State C described in that work is ν_{11}, the A_2 out-of-plane ring deformation mode without significant chlorine atom motion. State D is very likely ν_{15}, the B_1 out-of-plane ring deformation mode without significant chlorine atom motion. The observation of these states, particularly the modes corresponding to the out-of-plane ring deformation with chlorine motion and the in-plane bend of $\sigma_{C\text{-}Cl}$, is consistent with those observed in studies of other monosubstituted haloarenes [2,19]. Two states lower in energy (ν_9 and $\nu_{16} + \nu_{24}$), and thus more intense than ν_{15}, were not identified in the previous work [6].

As is clear from Table 8, the vibration-rotation interaction constants of the three lowest-energy fundamentals for chloropyrazine and 2-chloropyrimidine display remarkable similarity. The out-of-plane $\sigma_{C\text{-}Cl}$ bends (ν_{24} for chloropyrazine and ν_{16} for 2-chloropyrimidine) for each molecule have large impacts on A_v due to moving the chlorine atom off of the *a*-axis along with loss of ring planarity. These bends have a much smaller impact on B_v and C_v as the chlorine atom is already far from those axes and the motions of the ring atoms with respect to the *b*- and *c*-axes have a smaller effect. The in-plane $\sigma_{C\text{-}Cl}$ bends (ν_{17} for chloropyrazine and ν_{24} for 2-chloropyrimidine) move all of the atoms with respect to the *a*-axis, causing a large change in A_v with respect to their corresponding A_0 values. Similar to the lowest-energy states

Table 8
Comparison of experimental spectroscopic constants for [^{35}Cl]-chloropyrazine and [^{35}Cl]-2-chloropyrimidine [6] (A-reduced Hamiltonian, I^r representation).

	[^{35}Cl]-chloropyrazine		[^{35}Cl]-2-chloropyrimidine	
	Experimental	B3LYP/6-311+(2d,p)	Experimental [6]	B3LYP/6-311+(2d,p)
	ν_{24}		ν_{16}	
$A_0 - A_v$ (MHz)	28.6336 (22)	29.16	25.75 (5)	26.50
$B_0 - B_v$ (MHz)	−1.117171 (83)	−1.08	−1.360 (5)	−1.35
$C_0 - C_v$ (MHz)	−1.583008 (77)	−1.56	−1.8173 (22)	−1.80
	ν_{17}		ν_{24}	
$A_0 - A_v$ (MHz)	−25.1066 (21)	−25.97	−21.23 (6)	−22.12
$B_0 - B_v$ (MHz)	−0.115375 (73)	−0.06	0.008 (4)	0.06
$C_0 - C_v$ (MHz)	0.954345 (63)	1.05	1.0744 (32)	1.19
	ν_{23}		ν_{11}	
$A_0 - A_v$ (MHz)	4.5728 (21)	4.45	4.74 (8)	5.17
$B_0 - B_v$ (MHz)	−0.161208 (75)	−0.12	−0.237 (5)	−0.21
$C_0 - C_v$ (MHz)	−0.740197 (64)	−0.70	−0.829 (3)	−0.79
	ν_{16}		ν_9	
$A_0 - A_v$ (MHz)	0.3721 (23)	−0.44		−0.55
$B_0 - B_v$ (MHz)	1.530827 (74)	1.99		2.02
$C_0 - C_v$ (MHz)	0.842223 (66)	1.04		0.97
	ν_{22}		ν_{15}	
$A_0 - A_v$ (MHz)	1.504 (55)	1.69	0.32 (5)	0.01
$B_0 - B_v$ (MHz)	0.0042 (46)	0.12	0.354 (8)	0.45
$C_0 - C_v$ (MHz)	−0.682660 (84)	−0.67	−0.4961 (31)	−0.48

(ν_{24} and ν_{16}), the impact of these vibrations is much smaller on B_v and C_v. The set of third lowest-energy fundamentals (ν_{23} for chloropyrazine and ν_{11} for 2-chloropyrimidine) for each molecule involves another out-of-plane ring deformation, but this time with a relatively stationary chlorine atom compared to the lowest energy fundamentals (ν_{24} and ν_{16}). The relatively stationary chlorine atom showcases the impact of the out-of-plane motions of the ring atoms on the A_v constant value for those modes. Fundamental ν_9, though lower in energy than ν_{15}, is absent from the reported work on [^{35}Cl]-2-chloropyrimidine, so no comparison is available for the set of σ_{C-Cl} stretching modes (ν_{16} for chloropyrazine and ν_9 for 2-chloropyrimidine). These modes do have small observed changes in A_v relative to the changes in B_v and C_v due to the motion of the atoms nearly parallel to the *a*-axis. The final set of observed fundamentals (ν_{22} and ν_{15}, the fifth lowest-energy fundamentals) is similar to ν_{23} and ν_{11} in that they involve both out-of-plane ring deformations and small chlorine atom motions. As with those states, ν_{22} and ν_{15} have relatively small vibration-rotation interaction constants. Interestingly, these values exhibit the greatest percentage differences between analogous vibrations of each molecule. Inspection of the computational output reveals that all of the ring atoms are involved in the vibration for chloropyrazine, but that the nitrogen atoms of 2-chloropyrimidine are nearly stationary in this mode. As a result, the total of absolute displacements of all atoms is larger for ν_{22} of chloropyrazine than ν_{15} of 2-chloropyrimidine. This difference of vibrational motion is likely responsible for the observed difference in the vibration-rotation interaction constants for these fundamentals. For both molecules, the anharmonic frequency calculations at the B3LYP/6-311+G(2d, p) level satisfactorily predict the vibration-rotation interaction constants.

Acknowledgements

We gratefully acknowledge funding from the National Science Foundation for support of this project (NSF-CHE-1664912) and for support of shared Departmental computing resources (NSF-CHE-0840494). We thank Tanner M. Zimmerman for his work on the initial fitting of the [^{35}Cl]-chloropyrazine ground state. We thank Michael McCarthy for the loan of an Amplification-Multiplication Chain and Mark Wendt for the loan of an analog signal generator. We thank the Harvey Spangler Award (to B.J.E.) for the funding that supported the purchase of the zero-bias detector.

Declaration of Competing Interest

None.

Appendix A. Supplementary material

Supplementary data to this article can be found online at https://doi.org/10.1016/j.jms.2019.111179.

References

[1] B.J. Esselman, B.K. Amberger, J.D. Shutter, M.A. Daane, J.F. Stanton, R.C. Woods, R.J. McMahon, Rotational Spectroscopy of pyridazine and its isotopologs from 235–360 GHz: equilibrium structure and vibrational satellites, J. Chem. Phys. 139 (2013) 224304.
[2] O. Dorosh, E. Białkowska-Jaworska, Z. Kisiel, L. Pszczółkowski, New measurements and global analysis of rotational spectra of Cl-, Br-, and I-benzene: spectroscopic constants and electric dipole moments, J. Mol. Spectrosc. 246 (2007) 228–232.
[3] N. Heineking, H. Dreizler, Nitrogen and chlorine hyperfine structure in the rotational spectra of 4-chloropyridine, Z. Naturforsch., A 41A (1986) 1297–1301.
[4] M. Meyer, U. Andresen, H. Dreizler, Microwave spectrum and nuclear quadrupole coupling of 2-chloropyridine, Z. Naturforsch., A 42 (1987) 197–206.
[5] N. Heineking, H. Dreizler, Nuclear quadrupole hyperfine structure in the rotational spectrum of 3-chloropyridine. an application of microwave-microwave double resonance fourier transform spectroscopy, Z. Naturforsch., A 43 (1988) 657–661.
[6] C.D. Paulse, The Microwave Spectra of Two Halogenated Pyrimidines. M.S. Thesis, Chemistry Department, Memorial University of Newfoundland, St. John's, Newfoundland, Canada, 1990, p. 81.
[7] S. Akavipat, The Microwave Spectra of Chloropyrazine and Cycloheptanone. M. S. Thesis, Department of Physics, Mississippi State University, Mississippi State University, 1978, p. 73.
[8] S. Akavipat, C.F. Su, R.L. Cook, Microwave spectra of chloropyrazine, J. Mol. Spectrosc. 111 (1985) 209–210.
[9] H. Endrédi, F. Billes, S. Holly, Vibrational spectroscopic and quantum chemical study of the chlorine substitution of pyrazine, J. Mol. Struct. THEOCHEM 633 (2003) 73–82.
[10] B.K. Amberger, B.J. Esselman, J.F. Stanton, R.C. Woods, R.J. McMahon, Precise equilibrium structure determination of hydrazoic acid (HN_3) by Millimeter-wave spectroscopy, J. Chem. Phys. 143 (2015) 104310.
[11] M.A. Zdanovskaia, B.J. Esselman, R.C. Woods, R.J. McMahon, The 130–370 GHz rotational spectrum of phenyl isocyanide (C_6H_5NC), J. Chem. Phys. 151 (2019) 024301.
[12] Z. Kisiel, L. Pszczółkowski, B.J. Drouin, C.S. Brauer, S. Yu, J.C. Pearson, I.R. Medvedev, S. Fortman, C. Neese, Broadband rotational spectroscopy of acrylonitrile: Vibrational energies from perturbations, J. Mol. Spectrosc. 280 (2012) 134–144.
[13] Z. Kisiel, L. Pszczółkowski, I.R. Medvedev, M. Winnewisser, F.C. De Lucia, E. Herbst, Rotational spectrum of trans–trans diethyl ether in the ground and three excited vibrational states, J. Mol. Spectrosc. 233 (2005) 231–243.
[14] Z. Kisiel, E. Białkowska-Jaworska, Sextic centrifugal distortion in fluorobenzene and phenylacetylene from cm-wave rotational spectroscopy, J. Mol. Spectrosc. 359 (2019) 16–21.
[15] Gaussian 16, Revision B.01, M.J. Frisch, G.W. Trucks, H.B. Schlegel, G.E. Scuseria, M.A. Robb, J.R. Cheeseman, G. Scalmani, V. Barone, G.A. Petersson, H. Nakatsuji, X. Li, M. Caricato, A.V. Marenich, J. Bloino, B.G. Janesko, R. Gomperts, B. Mennucci, H.P. Hratchian, J.V. Ortiz, A.F. Izmaylov, J.L. Sonnenberg, D. Williams-Young, F. Ding, F. Lipparini, F. Egidi, J. Goings, B. Peng, A. Petrone, T. Henderson, D. Ranasinghe, V.G. Zakrzewski, J. Gao, N. Rega, G. Zheng, W. Liang, M. Hada, M. Ehara, K. Toyota, R. Fukuda, J. Hasegawa, M. Ishida, T. Nakajima, Y. Honda, O. Kitao, H. Nakai, T. Vreven, K. Throssell, J.A. Montgomery Jr., J.E. Peralta, F. Ogliaro, M.J. Bearpark, J.J. Heyd, E.N. Brothers, K.N. Kudin, V.N. Staroverov, T.A. Keith, R. Kobayashi, J. Normand, K. Raghavachari, A.P. Rendell, J.C. Burant, S.S. Iyengar, J. Tomasi, M. Cossi, J.M. Millam, M. Klene, C. Adamo, R. Cammi, J.W. Ochterski, R.L. Martin, K. Morokuma, O. Farkas, J.B. Foresman, D.J. Fox, Gaussian, Inc., Wallingford CT, 2016.
[16] J.R. Schmidt, W.F. Polik, WebMO Enterprise, WebMO, LLC., Holland, MI, USA, 2016.
[17] D. Papoušek, M.R. Aliev, Molecular Vibrational-Rotational Spectra, Elsevier, Prague, 1982, p. 170.
[18] J. Kraitchman, Determination of Molecular Structure from Microwave Spectroscopic Data, Am. J. Phys. 21 (1953) 17–24.
[19] Z. Kisiel, E. Białkowska-Jaworska, L. Pszczółkowski, The Millimeter-Wave Rotational Spectrum of Fluorobenzene, J. Mol. Spectrosc. 232 (2005) 47–54.